

Numerical Modelling of Effective Diffusivity in Bone Tissue Engineering

Ayesha Sohail, Khadija Maqbool, Anila Asif, Haroon Ahmad

Abstract—These days, the field of tissue engineering is getting serious attention due to its usefulness. Bone tissue engineering helps to address and sort-out the critical sized and non-healing orthopedic problems by the creation of manmade bone tissue. We will design and validate an efficient numerical model, which will simulate the effective diffusivity in bone tissue engineering. Our numerical model will be based on the finite element analysis of the diffusion-reaction equations. It will have the ability to optimize the diffusivity, even at multi-scale, with the variation of time. It will also have a special feature “parametric sweep”, with which we will be able to predict the oxygen, glucose and cell density dynamics, more accurately. We will fix these problems by modifying the governing equations, by selecting appropriate spatio-temporal finite element schemes and by transient analysis.

Keywords—Bone tissue engineering, Transient Analysis, Scaffolds, fabrication techniques.

I. INTRODUCTION

BONE “tissue engineering” is an extremely challenging field of research. The major steps involved in this study are (a) The osteo-progenitor cell mobility, (b) the proliferation process, (c) the differentiation, (d) the bone matrix formation. The major achievements in bone “tissue engineering” with the scaffolds are gained by use of drugs, gene deliveries and growth factors. These scaffolds are composed of porous degradable materials, which are involved during repair mechanism and regeneration process of infested bone. Scaffolds are commonly used to deliver bio-molecules in bone-tissue-engineering process. Khan et al. [1] discussed the numerous design considerations, which are relevant to successful bone repair with tissue-engineered matrices. An overview of several manufacturing techniques that allow for the actualization of significant design parameters is discussed in [1].

A scaffold is also pronounced as a three dimensional robust environment to facilitate elementary structure to pack the tissue material and supply cells a viable environment for the abundance and demarcation. Cell-seeded scaffolds can be cultured *in vitro* before implantation for few times. Most favorable approach on cell seeding into scaffolds is keen to gain accurate cell elongation in the scaffold entirely.

Jeong et al. [2] proposed an efficient mathematical modelling to predict the growth and distribution of cells

in scaffolds. They proposed that by using the numerical simulations, the experimental results could be interpreted to identify dominating mechanisms.

Cao and Kuboyama [3] investigated the PGA/beta-TCP scaffolds during the repair of critical bone defects (3 mm diameter, 2 mm depth) in rat femoral medial-epicondyles, compared with hydroxylapatite (HAP) and no implant as controls. They used the *in vivo* micro-CT images to perform the quantitative imageology analysis (i.e. volume and density of new bone) and qualitative histological evaluations (i.e. hematoxylin and eosin staining; tartrate-resistant acid phosphatase-hematoxylin counterstaining) at 0, 14, 30 and 90 days after surgery. Significant differences of all variables were tested by multivariate analysis ($p \leq 0.05$). With experimental evidence, it was showed that the bones reformed by using the PGA/beta-TCP scaffolds. The reformation began within 14 days of surgery, and bones were healing well at 30 days after surgery.

Herrera et al. [4] discussed in detail the modelling of scaffold. They concluded that once an internal properly inter-connected scaffold micro-structure is developed, the net rate of bone regeneration is very similar from one micro-architecture to another.

A bone scaffold has many requirements. One of them is bio-compatibility as it is the ability to maintain normal cell activity. Williams [5] discussed some properties of scaffold. A commercially ideal bone “scaffold should be osteo-conductive, i.e. it must have the ability to let the bone cells maintain their position (adhere) and broadcast a network on the surface of scaffold (matrix form). The youngest component of cortical bone ranged from 15 to 20 GPa, Cancellous bone is from 0.1 to 2 GPa and good strength from 100 to 200 MPa in cortical part of bone and ranged from 2 to 20 MPa. The large disparity in “mechanical characteristics” and shape makes it very complicated to build an “ideal scaffold” as discussed by Olszta et al. [6]. The size of pores matters a lot in scaffold study. The minimum pore size should be 100 μ m in size for accurate diffusion of necessary nutrients and O₂ for the growth and survival of cell. Meanwhile, the optimum range of pore size is from 200-350 μ m for bone tissue in-growth. Nowadays, it has been investigated that the combination of multi-scale and porous scaffolds can shows better results than, only the macro porous scaffolds [7]. The porosity reduces the mechanical properties like strength and enhances the complexity of scaffold. The scientist proposed porous scaffolds, by using ceramics, polymers and metals. These scaffolds should be compatible with the “mechanical” necessities of bone. Another key feature of an ideal scaffold is

Ayesha Sohail is with the Department of Mathematics, Defence Road off Raiwind road Lahore, Pakistan (e-mail:asohail@ciitlahore.edu.pk).

Khadija Maqbool is with the Department of Mathematics & Statistics, FBAS, IIUI, Islamabad 44000, Pakistan.

Anila Asif is with the Department of IRCBM, Defence Road off Raiwind road Lahore, Pakistan.

Haroon Ahmad is with the Department of Biosciences, COMSATS Institute Of Information Technology (CIIT), Park Road, Chakshazad, Islamabad.

spontaneous degradation, *in vivo*, preferably in the controlled resorption time and would be able to create maximum space for new bone to grow.

Geris et al. [8] emphasised on addressing an important issue, which is the clear understanding of interaction between experiments and simulation. In the topic areas of their review [8], most models are applied to already published data and experimental situations. In such articles, the authors reproduce the known experimental findings. Hence experimental results get linked with modelling. Authors then often use their models to also suggest improved treatment strategies to deal with, e.g., difficult healing cases. Whereas this predictive power of a model is customarily used in engineering applications. The predictive power of models still need to find their way back to the experimentalists and clinicians.

Scaffolds are planned with immixed porosity having osteogenic and angiogenic component were added. The organisation of porosity of scaffolds play an important role during bone formation. There are various fabrication techniques used now a days. From these various fabrication techniques, SFF dependent method is a famous technique for scaffold fabrication. 3D interconnected porous scaffolds ([9]-[12]).

Calcium phosphate (CaPs) is one of the major component of mammalian bone. That's why, the CaPs contributes a lot in bone tissue engineering study. During the past decades for designing the engineered bones, HA, *b*-TCP, BCP have been investigated extensively to formulate "porous scaffolds" such as studied by Rezwani et al. [13] and many more. For the preparation of the BCP-scaffold, one of the options is to use the polymer-replica technique.

Many different groups have been investigated in recent decade from the building of absorbable 45S5 Bioglass [14]. *In vitro* studies, a bio-glass 3-D scaffold with porosity of seventy percent, (300 to 400 mm size) having enhanced osteoblast activity due to the "hydroxy carbonate apatite (HCA)" layer can be formed. The advantage of this HCA layer is that it intake the bio-molecules ("protein and" "growth factors") and thus enhance the repaired bone formation *in vivo* [15].

In recent studies, "COBALT" was incorporated in bio-glass scaffolds (with intermediate sized pores) to produce low concentrated oxygen (hypoxia). It increases the "bone marrow-derived stem cell" (BMSC) expression, segregation process, discharge of (a) "VEGF", (b) "HIF-1 α ", and the allele-expression related to bone.

Bioactive and biodegradable polymers are widely used [16]. The silk, collagen, hyaluronic acid, fibrin, alginate and chitosan pure polymers for tissue engineering are commonly used. The PPF showed the very high compressive strength in comparison to cortical bone. The polymeric scaffolds show rapid strength degradation *in vivo* [17].

Composites are consisting of more than two distinctly different materials as ceramics etc. Polymer in "CaP scaffolds" Polymers play an important role to augment the stiffness and strength in CAP-scaffolds similar to bone. Meanwhile, "mechanical" stability and polymeric bio-activity could be enhanced by adding CAP. Majority of the "Porous metallic

scaffolds", were composed of Ti & Ta, have been widely studied as bone replacement materials due to rich compressive stability and good fatigue resistant [18].

CaP-scaffolds develop the fresh bone configuration and bio-mineralization, "Next generation scaffolds", are predicted to be osteo-inductive. Several methods have been used to form CAP-scaffold in a osteo-inductive typical feature, that is not restricted to improved scaffold chemistry. Osteo-induction is a process that is closely linked with both the pore size of material.

In all such scaffolds (made of different materials), an important point is the transport of the essentials to keep the seeded cells in scaffold alive. It is expensive to study the transport phenomena of the bio-materials through the structure of scaffolds *in vivo* and *in vitro*. To overcome this cost we have discussed the diffusion reaction equation and its transient analysis to address the functionality of an ideal scaffold.

II. PROBLEM STATEMENT

The bone-scaffolds are usually prepared of porous-degradable materials. One of the benefits of the scaffold implantation is to deliver bio-molecules such as proteins and growth factors including transferring augmentation factor (TGF- β), "bone morphogenetic protein (BMP)", Insulin-like augmentation factor (IGF) and fibro-blast "growth factor (FGF)". The mammalian bones are highly vascularized, therefore when a scaffold is implanted, it is desired that in a short time span, it will induce the formation of new blood vessels. The regular transport of the nutrients, oxygen and protein is essential for the better functionality of implanted scaffold. We have used a numerical finite element method based on backward difference scheme to demonstrate the transport of bio-molecules through the scaffold structure. We have developed a two dimensional (2D) model, in a manner similar to [19].

The numerical model is based on the following six steps: firstly we will define the model geometry based on the requirement of an ideal scaffold. This geometry will be built using the environment of a commercially available software Comsol multi-physics. While defining the geometry, a suitable mode of software will be chosen to provide the essential governing equations. The constants (model parameters) will be defined while designing the model. Next we will define the boundary conditions. The model domain will then be discretized by selecting a suitable mesh mode to acquire a desired accuracy. At the end we will run the numerical solver and will analyse the results for the concentration gradient. The convergent results will depend on two important features (a) the mesh statistics, and (b) the parametric sweep. A complete statistics will be provided to achieve better results.

A. Governing Equations

The main governing equation for the modelling of the bio-molecular transport through scaffold is the diffusion equation

$$\frac{\partial c^n}{\partial t} + \nabla \cdot (-D^n \nabla c^n) = 0 \quad (1)$$

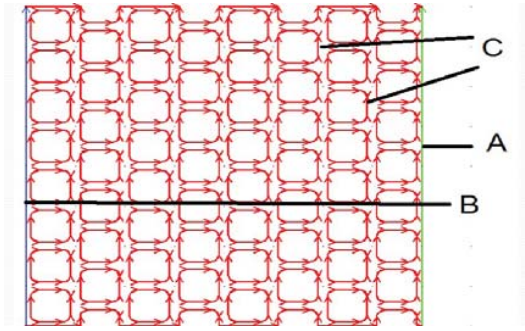


Fig. 1. Boundary Conditions.

where c is the concentration (mol/m^3), the superscript n varies from 1 to 3 for oxygen, glucose and nutrients. D^n is the diffusion coefficient (m^2/s). We have used this equation along with the equations at the boundaries of the scaffold, to model the diffusion. The first boundary condition is called the concentration boundary condition and is applied to the left boundary of the scaffold. It is expressed as

$$c^n = c_0^n \quad (2)$$

we have considered this condition at boundary B (see Fig. 1) The second boundary condition is the right vertical boundary and is set to be

$$(-D^n \nabla c^n) \cdot \mathbf{N} = k_m (c^n - c_1) \quad (3)$$

where k_m is the mass transfer coefficient (m/s). c_1 is the concentration in the bulk solution outside of the porous structure (see Fig. 1 boundary A). The third boundary condition is for the insulating boundary condition and is applied to boundaries of type C, (see Fig. 1 boundary C)

$$(-D^n \nabla c^n) \cdot \mathbf{N} = 0 \quad (4)$$

To model the homogenization and porosity, we have considered a model geometry with effective transport properties and average porosity. Keeping ξ as the average porosity and D_{ef}^n as the effective diffusivity (effective diffusion coefficient describes diffusion through the pore space of porous media).

The model equations can be written as

$$\xi \frac{\partial c^n}{\partial t} + \nabla \cdot (-D_{ef}^n \nabla c^n) = 0 \quad (5)$$

While modelling a porous scaffold, the most important issue is the detailed description of the flux. The mathematical approach to calculate the average flux is to integrate over the flux boundary and divide by its length. Our numerical model will calculate the flux and the concentration gradient.

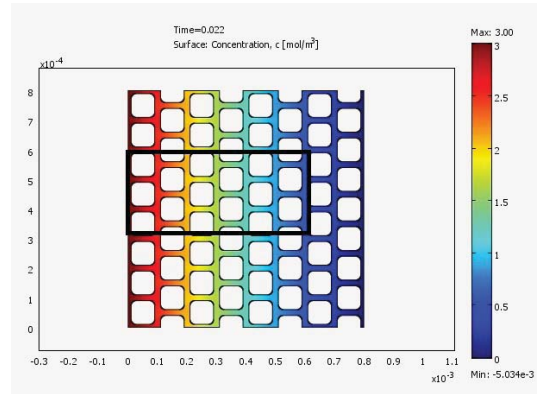


Fig. 2. Concentration Gradient.

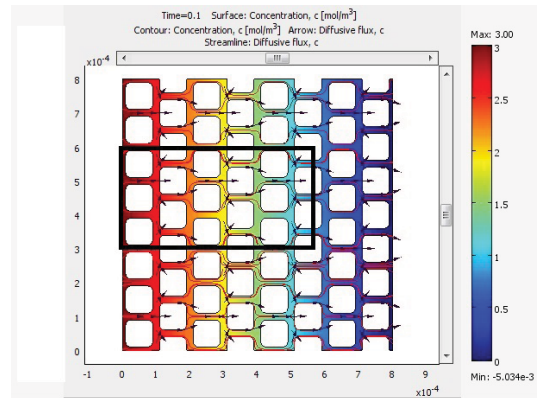


Fig. 3. Diffusive Flux Arrows.

B. Grid Convergence Analysis

We have first performed the grid convergence analysis to confirm the convergence of the numerical solver. We have solved the problem numerically for different degrees of freedom. The computational cost increased and the error decreased as we reduced the mesh size. Similar trend was observed by Sohail et al [20]. In Table I we have listed the ratio, the grid quality and the number of quadrilateral and triangular grids. In Table II we have listed the degree of freedom. We can see that for coarse (less DOF) the convergence rate is different from what is depicted from

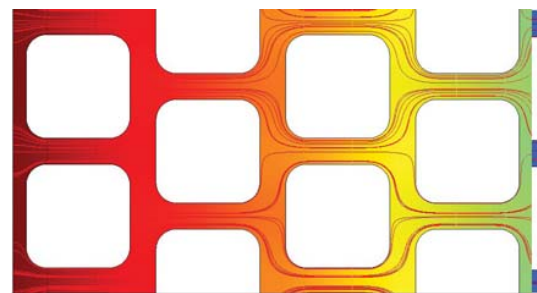


Fig. 4. Zoomed Region with Streamlines.

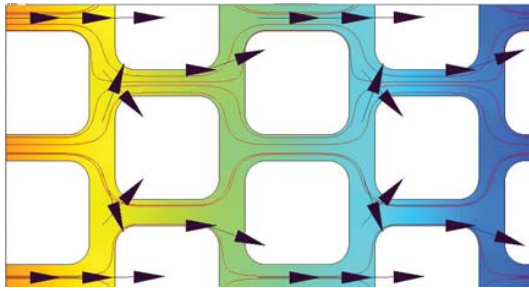


Fig. 5. Zoomed Region with Arrows of Diffusive Flux.

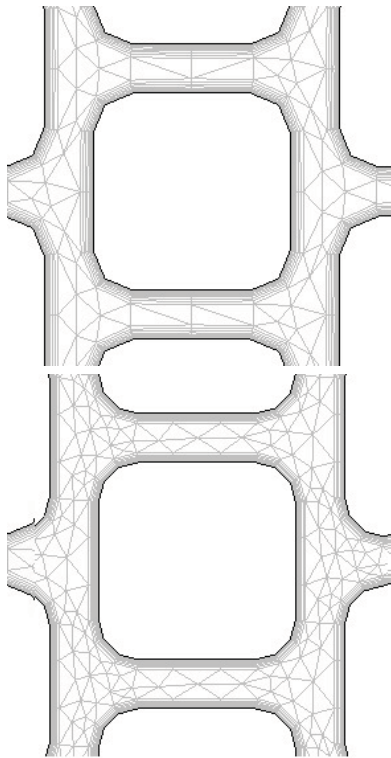


Fig. 6. Comparison of two Scaffold Pores Extra Coarse Mesh Mode and Coarse Mesh Mode.

finer mesh (higher DOF). The grid study helped to set up a numerical model for compatible shape and reasonable size of pores for better functionality of scaffold and for bone-repair. Since the human bones are highly vascularized, therefore from a smartly designed scaffold, it is desired that it will swiftly induce the formation of new blood vessels. This could be achieved by the regular transport of the nutrients, oxygen and protein through the scaffold structure. To understand this phenomena a detailed analysis of the discredited scaffold structure is discussed.

III. RESULTS AND DISCUSSION

We have performed a list of numerical experiments to achieve the required accuracy. We have presented the numerical results graphically and in tabulated form. We can

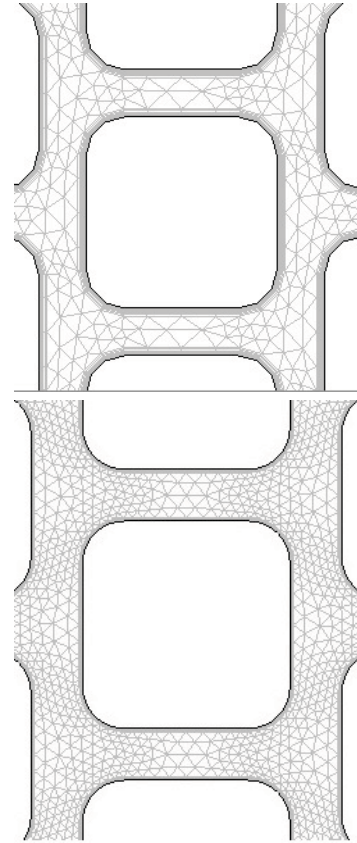


Fig. 7. Comparison of two Scaffold Pores Fine Mesh Mode and Extra Fine Mesh Mode.

see from these results that good convergence is achieved for the 2D analysis by taking into account the mesh statistics.

Fig. 2 depicts the concentration gradient in mol/m^3 at time $t = 0.022$ s. The colour bar represents here the concentration variation throughout the scaffold. We have declared in the model equations the indices for the oxygen, glucose and nutrients. Therefore we can trace out the gradients in these components during the bio molecular transport. Secondly the effective diffusivity near and far from the source wall is examined. We have showed the time dependance of the transport phenomena with the aid of images. The effective diffusivity and the flux are considered to demonstrate this phenomena.

From Fig. 3 we can depict the concentration gradient and the diffusive flux. The arrows represents the flux through the scaffold structure at time $t = 0.1$ s. To explain the change in concentration and the diffusive flux, we have presented the zoomed images (see Fig. 4 and Fig. 5)

Our future work will be focused to design a numerical 3D model, with more advanced features. We aim to address two main issues, the anisotropy and the adaptive mesh refinement in our future work. Our numerically obtained results for the flux and concentration gradients will help to predict the functionality of the scaffold *in vitro*.

TABLE I
NUMBER OF ELEMENTS AND THEIR CHARACTERISTICS

i	N_{ratio} 10^{-3}	$N_{quality}$ 10^{-2}	N_{Δ}	N_{\circ}
1	5.6	1.82	2657	10088
2	10.5	1.86	5862	14080
3	13.4	2.09	7334	16080
4	12.6	2.14	11042	20448
5	12.2	2.23	21181	29352
6	11.8	2.23	21257	29400
7	11.4	2.39	23426	33856
8	11.6	2.27	31224	36032
9	12.8	2.47	31502	40240

TABLE II
GRID CONVERGENCE ANALYSIS

i	DOF	nodes
1	46868	11988
2	69745	17832
3	80939	20693
4	106373	27188
5	163380	41718
6	163730	41807
7	186449	47626
8	211021	53837
9	228935	58447

REFERENCES

- [1] Khan, Y. et al. (2008) Tissue engineering of bone: material and matrix considerations. JBJS 90, 3642
- [2] Darae Jeong, Ana Yun, Junseok Kim. Mathematical model and numerical simulation of the cell growth in scaffolds. Biomech Model Mechanobiol (2012) 11:677688, DOI 10.1007/s10237-011-0342-y
- [3] Cao, H. and Kuboyama, N. (2010) A biodegradable porous composite scaffold of PGA/b-TCP for bone tissue engineering. Bone 46, 386395.
- [4] Sanz-Herrera, Jose A., Manuel Doblar, and Jos M. Garca-Aznar. Modelling bone tissue engineering. Towards an understanding of the role of scaffold design parameters. Advances on Modeling in Tissue Engineering. Springer Netherlands, 2011. 71-90.
- [5] Williams, D.F. (2008) On the mechanisms of biocompatibility. Biomaterials 29, 29412953.
- [6] Olszta, M.J. et al. (2007) Bone structure and formation: A new perspective. Mater. Sci. Eng. R: Rep. 58, 77116.
- [7] Woodard, J.R. et al. (2007) The mechanical properties and osteoconductivity of hydroxyapatite bone scaffolds with multi-scale porosity. Biomaterials 28, 4554.
- [8] Geris, Liesbet, Alf Gerisch, and Richard C. Schugart. Mathematical modeling in wound healing, bone regeneration and tissue engineering. Acta biotheoretica 58.4 (2010): 355-367.
- [9] Scaglione, S. et al. (2012) Order versus disorder: in vivo bone formation within steoconductive scaffolds. Sci. Rep. 2, Article no. 274.
- [10] Bose, S. et al. (1999) Processing of controlled porosity ceramic structures via fused position. Scripta Mater. 41, 10091014.
- [11] Darsell, J. et al. (2003) From CT scan to ceramic bone graft. J. Am.Ceram. Soc. 86, 10761080.
- [12] Hutmacher, D.W. et al. (2004) Scaffold-based tissue engineering:rationale for computer-aided design and solid free-form fabrication systems. Trends Biotechnol. 22, 354362.
- [13] Rezwan, K. et al. (2006) Biodegradable and bioactive porous polymer/inorganic composite scaffolds for bone tissue engineering. Biomaterials 27, 34133431.
- [14] Jones, J.R. et al. (2006) Optimising bioactive glass scaffolds for bone tissue engineering. Biomaterials 27, 964973.
- [15] Miguel, B.S. et al. (2010) Enhanced osteoblastic activity and bone regeneration using surface-modified porous bioactive glass scaffolds. J. Biomed. Mater. Res. Part A 94A, 10231033.
- [16] Lichte, P. et al. (2011) Scaffolds for bone healing: concepts, materials and evidence. Injury 42, 569573.
- [17] Bose S, Roy M, Bandyopadhyay A. Recent advances in bone tissue engineering scaffolds. Trends in biotechnology 2012;30(10):546-554. doi:10.1016/j.tibtech.2012.07.005.
- [18] Dabrowski, B. et al. (2010) Highly porous titanium scaffolds for orthopaedic applications. J. Biomed. Mater. Res. Part B: Appl. Biomater. 95B, 5361.
- [19] Guide, COMSOL Multiphysics UserS. "Comsol." Inc.-2006.-708 p (1994).
- [20] Sohail, Ayesha, Hafiz Abdul Wajid, and Mohammad Mehdi Rashidi. "Numerical Modeling Of CapillaryGravity Waves Using The Phase Field Method." Surface Review and Letters (2014).

ACKNOWLEDGMENT

The authors would like to thank Pakistan Science Foundation for grant PSF P and D TG II (1354) 14.